

On the Nature of Energy Transfer at Low Temperatures in the BChl *a* Pigment–Protein Complex of Green Sulfur Bacteria

R. J. W. Louwe and T. J. Aartsma*

Department of Biophysics, Huygens Laboratory, Leiden University, P. O. Box 9504,
2300 RA Leiden, The Netherlands

Received: October 29, 1996; In Final Form: February 21, 1997[⊗]

The technique of accumulated photon echoes was used to study optical dephasing of the lowest Q_Y transitions of the bacteriochlorophyll *a* complex of the green sulfur bacteria *Prosthecochloris aestuarii*. Variations in the photon echo decay as a function of wavelength are interpreted in terms of (phonon-assisted) downward relaxation within the Q_Y manifold as a mechanism of energy transfer at the lowest temperatures. A temperature dependence study revealed contributions to the total dephasing both from transitions within so-called two level systems (TLS) of the host as well as activation of transitions to higher electronic levels within the Q_Y manifold at temperatures above 5 K. Conclusions are drawn about the nature of energy transfer at low temperatures.

Introduction

Energy transfer has already been a subject of interest for many years and often a distinction is made between the weak coupling case and the strong coupling case, usually referring to the strength of the (dipolar) interaction between the pigments relative to the strength of the electron–phonon coupling. A more general description of the energy transfer process is offered by the generalized master equation (GME) or the (equivalent) stochastic Liouville equation (SLE)¹ approach. It has been shown that these theories represent a unifying approach, comprising both limiting cases.^{2–4}

For energy transfer in photosynthetic antenna systems, where the intermediate coupling case might be applicable, however, the situation is complicated due to several factors. Although some antenna systems possess a high degree of symmetry,⁵ reflected in specific properties of the electronic hamiltonian of the system and of the electronic transitions, this high degree of symmetry is not a general feature of antenna systems (see, e.g., refs 6–8). In particular, in the case of low symmetry, variations in site energy are to be expected which are not known a priori and will be comparable to or even larger than the strength of the interaction between the individual pigments.⁹ Furthermore, the various spectra of the electronic transitions of these systems are characterized by a large inhomogeneous broadening. Concerning the broadening mechanisms, usually a distinction is made between static and dynamic processes, reflecting inhomogeneous and homogeneous broadening of the electronic transitions, respectively. Both can be subdivided further into local processes, modulating the site energies of the individual pigments, and nonlocal processes, modulating the strength of the interaction between the pigments. Recent dephasing and spectral diffusion studies on various pigments in glasses, polymers, and proteins show that relaxation processes of these amorphous solids occur on all time scales.^{10–13} In antenna systems these fluctuations of the site energies will be observable as fluctuations of the eigenenergies of the system on all time scales and therefore a general distinction between dynamic and static processes should not be made without considering the time scale of the experiment. Due to all these complicating factors, a full description of energy transfer in photosynthetic

antenna systems using the SLE or GME is a formidable task. The (in-)coherent nature of the energy transfer mechanism in photosynthetic antenna systems is still a subject of discussion, often based on experiments which do not measure the coherence of the excited states directly.

All these considerations prompted us to measure the coherence directly using the accumulated photon echo technique to gain more insight in the coherence of energy transfer. In this article we present data on the BChl *a* pigment–protein complex from green sulfur bacteria, often referred to as the Fenna–Matthews–Olson (FMO) complex. The structure of this pigment–protein complex has been elucidated by X-ray crystallography with near atomic resolution^{7,8} and it consists of three subunits in C_3 symmetry, whereby each subunit contains seven BChl *a*'s. The nearest-neighbor distance between the BChls within each subunit is on the average about 12 Å and that between BChls belonging to different subunits 24 Å, yielding interactions between the BChls with a maximum of approximately 200 cm^{−1} and 20 cm^{−1}, respectively.

The FMO-complex has been fairly well characterized spectroscopically^{14–17} and shows a well-resolved Q_Y absorption region at cryogenic temperatures in optical steady state spectra. The absorption spectrum and circular dichroism spectrum can be simulated reasonably well by using exciton theory.^{18,19} So far, it has been impossible, however, to obtain a set of parameters for this model that would simulate the linear dichroic (LD), the triplet minus singlet ($T - S$), and the linear dichroic triplet minus singlet ($LD-(T - S)$) spectra simultaneously to the same degree of accuracy.²⁰

Time-resolved spectroscopy has mostly been applied at room temperature^{21–25} on different time scales and indicates that thermal equilibration and probably localization of an excitation to the lowest energy state of the complex occurs in less than 1 ps, although the time constants found in the different experiments vary somewhat. At lower temperatures such studies are rather scarce. At 77 K, Zhou et al.²⁵ showed that the fluorescence decay was dominated by a component with a time constant of 2 ns. Very recently, Savikhin and Struve²⁶ presented results of transient absorption experiments on the FMO-complex of *Chlorobium tepidum* at 19 K, showing that thermal equilibration in the Q_Y manifold slows down by almost 2 orders of

* Author to whom correspondence should be addressed.

⊗ Abstract published in *Advance ACS Abstracts*, August 1, 1997.

magnitude in going from 300 K to 19 K; decay to the ground state occurred with a time constant of ~ 1 ns at 829 nm.

Johnson and Small performed persistent hole-burning experiments on the FMO-complex at 4.2 K,²⁷ reporting only two distinct holewidths. Narrow holes of 0.5 cm^{-1} width, limited by spectral resolution, were observed in the long-wavelength region (around 825 nm) of the Q_Y absorption band. Below 820 nm only 50-cm^{-1} -wide holes were reported, assumed to be evidence for fast relaxation in this wavelength range. Satellite holes at higher energies (relative to the burn frequency) were interpreted in terms of an exciton picture for this system as calculated by Pearlstein.¹⁸

In this article we present (one color) accumulated photon echo measurements on FMO, determining the coherence lifetime of the excited states directly. A study of the temperature dependence of the photon echo decay allows us to identify the dominant mechanisms in the dephasing of the electronic transitions. Furthermore, we are able to answer the question to what extent energy transfer should be regarded as a coherent or an incoherent process in this system.

Materials and Methods

Accumulated photon echo experiments were performed in the Q_Y absorption range around 810 nm of the BChl *a* pigment-protein complex of the green sulfur bacterium *Prosthecochloris aestuarii* at 1.4 K in a home built liquid He-bath cryostat. Experiments between 5 and 30 K were done in a helium flow cryostat (Oxford Instruments, Model CF1024). The samples were prepared similarly as described in ref 28 and had an o.d. of 1 in a 2-mm cuvet at 812 nm at room temperature. The sample contained 66% v/v glycerol to prevent cracking upon cooling and was degassed in an ultrasonic bath prior to cooling. The setup for the accumulated photon echo experiments is described in ref 29 and for the transient absorption measurements in ref 30. The data were fitted using a global analysis program based on the procedure described in ref 31. Moreover, each echo decay was fitted with a convolution of the instrument response function with a sum of exponentials. The instrument response function was determined by measuring an accumulated photon echo "decay" at elevated temperature, when the dephasing is very fast compared to the time resolution. The instrument response function could very well be fitted with a sech^2 shaped pulse corresponding to a typical pulse duration of 2 ps, depending somewhat on the alignment of the dye laser. We have also performed some accumulated photon echo experiments with stochastic excitation³² to obtain a better time resolution (as high as 300 fs), but this limits the wavelength selectivity in the experiment. To prevent photodamage of the sample the energies of the "pump" and "probe" beams were kept sufficiently low, typically 500 and $50\text{ }\mu\text{W}$, respectively. This corresponds to 6×10^{11} photons/ cm^2 and less than 3×10^{-3} photons per trimer per excitation pulse.

Results

Wavelength Dependence of the Accumulated Photon Echo Decays. The accumulated photon echo (APE) decays at 1.4 K in FMO are characterized by time constants ranging from subpicoseconds at the shortest wavelengths to several hundred picoseconds at the longest wavelengths (Figure 1). The individual echo traces at all wavelengths are multiexponential and can be fitted by a convolution of the instrument response function with a sum of at least two exponentials at the longest wavelengths, while at shorter wavelengths at least three or four exponentials are required. If the time constants are not constrained, the different fits of the echo traces at the various

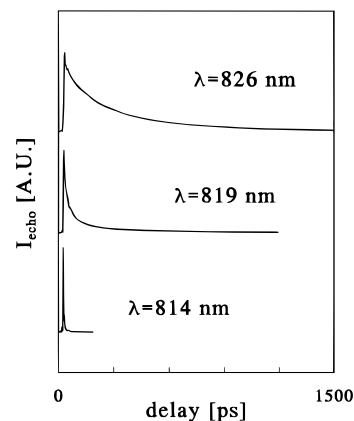


Figure 1. Typical accumulated photon echo of the FMO-complex traces recorded at three different wavelengths in the Q_Y absorption band, at 1.4 K.

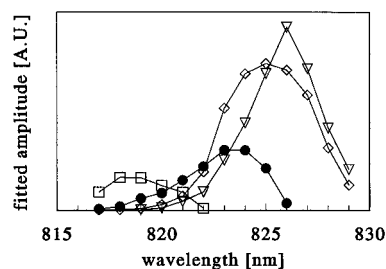


Figure 2. Decay associated spectrum of amplitudes associated with the time constants used to fit the APE traces of FMO recorded at 1.4 K. Time constants associated with each spectrum are as follows: (\square) 5 ps, (\bullet) 30 ps, (\diamond) 110 ps, and (∇) 385 ps.

wavelengths yield a consistent set of time constants within the experimental error. Using global analysis, time constants of 385, 110, 30, and 5 ps with an accuracy of $\pm 5\%$ could be resolved in the range 815–830 nm. At 815 nm and at wavelengths shorter than 815 nm we cannot unambiguously determine the fastest time constants, due to the fact that the dephasing rates at these wavelengths exceed the time resolution. However, we observed that also below 815 nm the overall photon echo decay time decreases from picoseconds at 815 nm to several hundred femtoseconds at 795 nm. The latter decay time was determined by stochastic excitation³² and represents the actual time resolution of that experiment. It provides an indication for the time scale of dephasing at this wavelength. A plot of the amplitudes versus excitation wavelength (decay associated spectrum, DAS) shows that each time constant is associated with a distinct spectral band (Figure 2). The bands are centered around 827, 826, 824, and 818 nm, and all have a width of approximately 75 cm^{-1} . In a preliminary study³³ at a higher temperature (5 K) we obtained somewhat shorter time constants of 250, 75, and 12.5 ps for the longest wavelength region with similar DAS,³⁴ indicative of an increased rate of dephasing.

Note that the time constants from the fits of the APE traces represent the total dephasing times T_2 divided by 2, since the measured intensity is proportional to the amplitude of the echo signal.³⁵ In none of the photon echo decay curves could an ultrafast decay component be distinguished within the signal to noise ratio. Such a component is very pronounced in APE decays of the primary donor of isolated reaction centers of purple bacteria³⁶ and stems from the contribution of the phonon sideband.³² These observations are consistent with the strength of the electron-phonon coupling, which is low in the FMO-complex and high in reaction centers, as was determined on the basis of various persistent holeburning measurements.^{27,37}

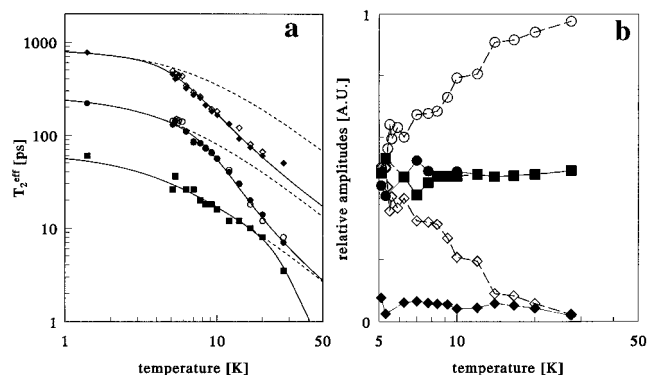


Figure 3. (a) Temperature dependence of the effective dephasing time constant T_2^{eff} determined from fits of individual APE traces at 821 and 826 nm. The solid lines represent fits of the data according to eq 1, while the broken lines represent the fits obtained by omitting the exponential term in this equation. Open markers, 826 nm; closed markers, 821 nm. (b) Relative contributions of the exponential terms to the fits.

Temperature Dependence of Dephasing. Since each dephasing mechanism has a characteristic temperature dependence, a temperature study can be used to gain insight in the different processes responsible for the optical dephasing in FMO. To that end, accumulated photon echo traces were measured as a function of temperature between 1.4 and 30 K at 821 and 826 nm. When the temperature is increased from 1.4 K, the dephasing at both wavelengths becomes significantly faster. At each temperature, the decays at both wavelengths can be fitted with two identical time constants within the experimental error, except that for the decays at 821 nm an additional time constant is needed (Figure 3a). We would like to emphasize that this is consistent with the APE results at 1.4 K, where identical time constants are found at adjacent wavelengths. In contrast to alternative sets of time constants, the set of time constants which is used here to describe the temperature dependence of dephasing yields a more or less smooth temperature dependence of the relative contributions of the exponential terms to the photon echo decays (Figure 3b). This observation has been taken into consideration to arrive at a final set of time constants. The fact that these relative contributions depend on temperature might indicate that the probability of localization of the triplet state on a specific pigment within the complex changes in this temperature region. Since the degree of participation of a specific pigment differs for each eigenstate, an alteration in the bottleneck state in an APE experiment will immediately affect the relative signal amplitudes of the various transitions. The limited number of data points prohibits a more rigorous analysis, however.

The temperature dependence of the total dephasing times can be fitted with a power law,³⁸ combined with an exponential activation of transitions to levels at higher energies:³⁹

$$\frac{1}{T_2} = \frac{1}{2T_1} + aT^\alpha + b \frac{e(-\Delta E/kT)}{1 - e(-\Delta E/kt)} \quad (1)$$

The parameters used in these fits are summarized in Table 1. The first term is due to population relaxation and is normally considered to be temperature independent. The second term in this equation describes the pure dephasing contribution due to transitions of two level systems (TLS), characterizing the dynamic properties of the protein. Such a power law has already been observed for various guest molecules in glasses, polymers, and proteins (see, e.g., refs 12, 38, and 40). The third term in eq 1 is used to describe a thermally induced activation process.

TABLE 1: Central Wavelengths λ_{DAS} of the Bands in the DAS, Expressed in Units of Energy and Their Mutual Energy Difference, ν_{DAS} and $\Delta\nu$, Respectively, and Parameters Used in the Fit of the Temperature Dependence of the Total Dephasing Time for the Lowest Transitions in the Q_Y Manifold of FMO (eq 1)

λ_{DAS} , nm	ν_{DAS} , cm^{-1}	$\Delta\nu$, cm^{-1}	T_1 , ps	a , $\text{ns}^{-1} \text{K}^{-\alpha}$	α , —	b , ns^{-1}	ΔE , cm^{-1}
827	12 091.9	14.6	420	0.09	1.3	23.6	15
826	12 106.5	29.4	135	0.44	1.3	377	29
824	12 135.9	89	32	2.20	1.3	47125	120
818	12 224.9						

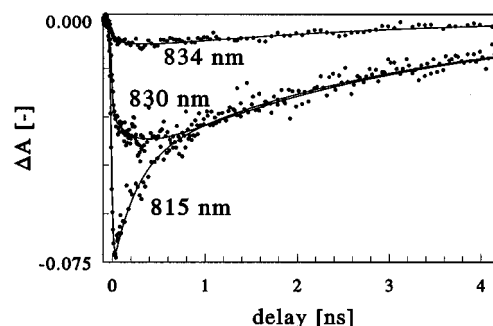


Figure 4. Transient absorption of the FMO-complex at 5 K. Excitation at 532 nm; probe wavelength 815, 830, and 834 nm. Pulse duration 35 ps.

We ascribe this activation process to population transfer between electronic levels within the Q_Y manifold (see Discussion). In Figure 3a the solid lines represent the fit of the temperature dependence according to eq 1, while the dashed lines are fits obtained by excluding the last term of eq 1. It can be seen that for all transitions the different fits only deviate at temperatures above 5 K, showing that thermal activation of transitions to other levels becomes important as a dephasing mechanism above this temperature.

Transient Absorption Measurements. The longest population lifetime of 420 ps in FMO implied by the fit of the temperature-dependent dephasing rates in the previous section (see also Table 1) is significantly shorter than the fluorescence lifetime observed in ref 25 for this system at 77 K.

To check whether this discrepancy is due to differences between our sample preparation and that of ref 25, transient absorption measurements at 5 K were performed at 815, 830, and 834 nm (Figure 4) with a time resolution of 25 ps. At all wavelengths time constants of 250 ps and 3 ns are found by using global analysis, although the sign of each component is different at the various wavelengths. At 830 and 834 nm a rise time of the bleaching is observed with a time constant of 250 ps, after which the signal decays with a time constant of approximately 3 ns. At these wavelengths the signal is dominated by stimulated emission, since the absorption of the sample is negligible and therefore the observed kinetics can be assigned to population relaxation to and from the lowest level of the Q_Y manifold of the complex. This assignment is consistent with the observed bleaching recovery at 815 nm with components of 250 ps and 3 ns. We note that the value of 3 ns is much longer than the value obtained from the fit of the temperature-dependent dephasing (420 ps) and is comparable to the observed fluorescence lifetime at 77 K.²⁵ The value of 994 ps as longest time constant found in transient absorption experiments in ref 26 is not very accurate, due to the relatively short time window of 590 ps in that particular experiment. Furthermore, it is questionable whether or not the contribution of single-triplet annihilation in these experiments can be ruled out. Anyhow, it is clear that a relaxation time derived from

the APE measurements is shorter than expected on the basis of the various T_1 -type experiments. Therefore we conclude that the APE time constants contain a contribution of spectral diffusion and that these time constants represent the so-called effective total dephasing time (see, e.g., ref 13).

Discussion

Dephasing Mechanisms in the FMO-Complex. An important difference between APE measurements on an antenna complex consisting of several interacting pigments as presented here and those on (monomeric) guest molecules in a host material is the possibility to stimulate an accumulated photon echo from different electronic transitions within the Q_Y manifold. This can be understood by realizing that the bottleneck state, necessary for accumulated photon echoes, is provided by the formation of a triplet state located on one of the pigments in the complex. The formation of such a triplet state results in a large shift of the site energy of that particular pigment and a vanishing of the dipolar interaction energy between that pigment and the others. These changes upon triplet formation shift all the electronic transitions of the complex. This is evident from an inspection of the T – S spectrum in the Q_Y region, which has a similar width as the corresponding absorption spectrum in this region.^{17,41} Due to this mechanism it is possible to create a so-called frequency grating at the excitation wavelength, from which an echo can be stimulated, even if the population of the bottleneck state occurs from another state within the Q_Y manifold than that which was directly excited. It is important to realize that even under saturating conditions, singlet–triplet annihilation does not contribute to the frequency grating and that the APE signal is therefore not influenced by this process. For a more extensive discussion on this subject we refer to a forthcoming paper on APE results on various antenna complexes of green plants.⁴²

Due to the inhomogeneous broadening, there will be an overlap of different transitions at a specific wavelength resulting in a simultaneous observation of accumulated photon echoes stimulated from different electronic transitions. We therefore interpret the multiple time constants of the individual APE decays as representing the time constants for dephasing of adjacent electronic transitions. Each time constant is associated with a distinct spectral band as shown in the DAS (Figure 2), presumably reflecting the inhomogeneous broadening of each transition. As mentioned before, the time resolution is not sufficient to uniquely determine the time constants for dephasing in the spectral region below 815 nm. In APE measurements it is possible to increase the time resolution by detuning the dye-laser cavity length, resulting in non-transform-limited pulses. Since only the coherent part of the pulse train contributes to accumulation of the population grating, this will effectively result in an increased time resolution, although at the expense of the spectral resolution. Obviously, the advantage of an improved time resolution in the global analysis procedure is eliminated by an increase of the number of time constants due to (a) the increased bandwidth of excitation and (b) an increasing density of states toward shorter wavelengths. Furthermore, a change of the coherence time generally yields a different contribution of spectral diffusion⁴³ and this may result in observation of different time constants, although this will mainly affect the longest time constants.

Given the weak electron–phonon coupling in the FMO complex, optical excitation predominantly populates the zero-phonon states of the Q_Y manifold. At the lowest temperatures used in the experiments, phonon-induced processes are virtually eliminated. Under these conditions it is appropriate to use a

description of energy transfer in terms of the basis set of (formally) delocalized eigenfunctions of the complex, since the measurements we present involve transitions between these eigenstates. In this representation, (phonon-assisted) downward relaxation within the Q_Y manifold is the main mechanism of energy transfer at the lowest temperatures, while at elevated temperatures, phonon-induced scattering between the electronic levels can act as an additional mechanism of energy transfer. The decrease of the dephasing time at 1.4 K toward shorter wavelengths presumably reflects the increasing number of relaxation paths for excitations at the higher levels in the Q_Y manifold. This part of the dephasing of each transition represents the temperature-independent population relaxation term T_1^{-1} in equation 1. From this equation it can be seen that apart from this population relaxation process, the dephasing of each transition also involves two temperature-dependent processes, described by a power law and an exponential activation term, respectively.

The dephasing mechanism described by the power law is typical for amorphous systems and can be theoretically explained^{44,45} in a model where a group of TLS are coupled to a guest molecule and the TLS are in turn coupled to the phonon bath. The TLS are related to different conformational (sub-)states¹¹ and transitions within the TLS, induced by the phonon bath, are responsible for fluctuations of the individual transition energies of the chromophores (local processes) and thus for fluctuations of all the eigen transitions of the complex in which those chromophores participate. This is similar to the fluctuation of the optical transition frequency of monomeric guest molecules in amorphous hosts. In the case of antenna complexes, however, fluctuations of the (dipolar) interaction between the pigments due to transitions within the TLS have to be considered as an additional dephasing (nonlocal) process. The transition rates of these TLS span a wide range of frequencies, and with respect to the distinction into local and nonlocal dephasing processes it might be expected that, in particular, TLS transitions with low frequencies (characterizing transitions between conformational states involving a relatively large displacement of the protein) may contribute more to modulation of the dipolar interaction energies, while the TLS transitions with high frequencies (with a corresponding smaller displacement of the protein) are more effective in modulation of site energies.

Due to the fact that the TLS's span a wide range of frequencies, the dephasing times (or homogeneous linewidths) obtained with different techniques depend on the time scale of the measurement (see, e.g., refs 38, 13, and 11). This dependence is commonly attributed to spectral diffusion and could be a reason for the discrepancy between the T_2 values we obtained and those from persistent hole-burning experiments reported in ref 27. In ref 27 it was claimed that dephasing in the Q_Y absorption band of the FMO complex occurs with a time constant of less than 100 fs at all wavelengths shorter than 820 nm, contrary to our observations. To resolve this discrepancy, holeburning in this wavelength region was recently also performed in our laboratory with a limiting spectral resolution of 0.2 cm^{-1} .⁴⁶ Most of the observations by Johnson and Small were reproduced, but also some differences were found. On the basis of these experiments, however, the hole burning data were reinterpreted with conclusions which are in good agreement with the accumulated photon echo measurements and also with pump–probe measurements at low temperatures.⁴⁷

Since there is a more or less continuous distribution of TLS transition frequencies, it is formally not correct to make a distinction between homogeneous and inhomogeneous broaden-

ing mechanisms. The broadening mechanisms which are static on the time scale of our experiment contribute to the Gaussian bands in the DAS and are thus observed as inhomogeneous broadening but are not necessarily static in the general sense. Broadening mechanisms which are not static on the time scale of our experiment are observed as a contribution to the homogeneous linewidth, reflected as a decrease of the dephasing time due to spectral diffusion. The time scale (often referred to as waiting time T_W) of an APE experiment is still a subject of discussion.^{10,12} Theoretically, the time scale is expected to be the lifetime of the bottleneck state (in our case the triplet state),⁴³ but spectral diffusion studies on ZnP in EtOD¹² and on myoglobin¹⁰ showed that the effective waiting time may be much shorter in amorphous solids.

As already described above, extrapolation of the fits of the temperature dependence of T_2 to 0 K yields population relaxation rates of 420 and 135 ps for the two lowest transitions. These values are significantly smaller than the values obtained with the transient absorption measurements (3 ns and 250 ps) and time resolved fluorescence at 77 K (2 ns).²⁵ This is an indication that spectral diffusion probably contributes considerably to the longest time constants for dephasing which we observe in accumulated photon echo measurements (see also below).

By analogy to other systems, the dephasing mechanism described by the exponential activation term in eq 1 might reflect either a librational motion as observed in various dimers in crystalline host materials,⁴⁸ activation of a narrow band optical phonon of the host as observed in glasses,^{49,50,12} or activation of a transition to another electronic level.⁵¹ In particular, scattering from the lowest to the upper dimer exciton level induced by linear electron–phonon coupling in mixed crystals of naphthalene dimers in perdeuteronaphthalene⁵² gave rise to an exponential temperature dependence of the photon echo decay. By similarity, the activation energies ΔE necessary to describe the temperature dependence of the dephasing time constants in our measurements match the separation in energy $\Delta\nu$ between the lowest electronic levels as found in the DAS (see Table 1) very well. Therefore we believe that all the dephasing processes described with an exponential law mainly represent activation of transitions to higher electronic levels within the manifold. Considering a possible involvement of processes reflecting a librational motion or activation of a narrow band optical phonon, it may be pointed out that, if the dephasing would depend on these processes, the activation energies would be similar for all the levels in the Q_Y manifold. Note, that the temperature dependence of the level centered at 12 121 cm^{-1} (824 nm) is very well described up to 25 K with a power law only and the activation energy for this level is substantially higher than that of the other levels, in agreement with the large energy gap with the level above it (see Table 1). From this variation in activation energy we conclude that it is unlikely that activation of a librational motion of the guest molecule or coupling to a narrow-band optical phonon of the host is involved in the temperature-induced dephasing.

Coherence of Energy Transfer. In the previous subsection we identified two mechanisms of energy transfer in the FMO-complex. At the lowest temperatures only downward energy transfer takes place, while at elevated temperatures scattering toward higher electronic levels becomes more important. Concerning the coherent nature of energy transfer we would like to emphasize that this property is obviously temperature dependent, as reflected by the temperature dependence of the total dephasing time (eq 1). To facilitate the discussion, we define the ratio c as a measure for the coherence of energy transfer:

$$c = \frac{T_2}{2T_1} \quad (2)$$

In the limit $T \rightarrow 0$ K the pure dephasing contribution to the total dephasing time is zero and energy transfer is completely coherent ($c \rightarrow 1$), while at elevated temperatures the pure dephasing contribution exceeds that of population relaxation to the total dephasing time, and energy transfer becomes incoherent ($c \rightarrow 0$). Obviously the parameter c becomes meaningless in the case of a very weak dipole–dipole interaction between the chromophores, and the eigenstates of the complex are more properly described as localized eigenstates. We assume, however, that this is not the case at the lowest temperatures and that (the temperature dependence of) the parameter c places an upper limit on the coherence of energy transfer. To obtain a relevant number for the ratio c , T_2 values as determined by e.g., two pulse echoes (TPE) should be used. For TPE the waiting time T_W is zero and therefore this technique yields T_2 values which are not affected by TLS flipping at rates slower than the time scale of energy transfer.

The question now arises how spectral diffusion influences the values for the pure dephasing time T_2^* and the total dephasing time T_2 as determined by a technique with a longer waiting time, $T_2^{*\text{eff}}$ and T_2^{eff} , respectively. Using nonlinear response theory, Bai and Fayer⁴³ found that spectral diffusion induces a factor, depending on the waiting time, between the T_2^* values observed with TPE and APE, but they did not consider explicitly the temperature dependence. In a study on the temperature dependence of spectral diffusion, the group of Völker⁵³ found that the temperature dependence of the inverse total effective dephasing time as observed with transient as well as permanent holeburning on BChl *a* in various solvents can be described with a power law $T^{1.3}$ and always extrapolates to the fluorescence lifetime limited value for $T \rightarrow 0$ K. Also in refs 12 and 54 a logarithmic plot of the pure dephasing time as a function of temperature shows parallel data sets for results obtained with TPE and APE. These observations are at variance with the temperature dependence of the 827-nm transition (upper trace in Figure 3a), which does not extrapolate to the expected fluorescence lifetime limited value. At present we have no explanation for this result. Nevertheless, we will make an estimation of the ratio c for this transition and for the transitions at 826 and 824 nm. To this end, we calculate c by dividing the observed dephasing time constants, T_2^{eff} , by the “lifetime limited values” from the fit parameters in Table 1, T_1^{eff} . By doing this we assume that T_1^{eff} and T_1 deviate by the same factor as T_2^{eff} and T_2 . Since the transitions toward shorter wavelengths have smaller dephasing times compared to that of the 827-nm transition, the relative contribution of spectral diffusion to those dephasing times is much smaller than to that of the 827-nm transition. We therefore estimate that this procedure yields reasonably accurate c values for the transition at 824 nm. For the 827-nm transition we consider the values for c as an upper bound to the degree in which energy transfer can be considered as coherent.

Plotting c as a function of temperature, the most striking observation is that c shows a similar behavior for all three transitions (Figure 5). Keeping in mind that $c = 0.5$ is a measure for the limit between coherent and incoherent energy transfer, Figure 5 shows that energy transfer in FMO is probably only coherent at temperatures below 5 K. As mentioned before, the dephasing due to scattering between the electronic levels as described by an exponential law becomes appreciable only at temperatures above 5 K. We tentatively conclude, therefore, that even when the activation energies for this dephasing process

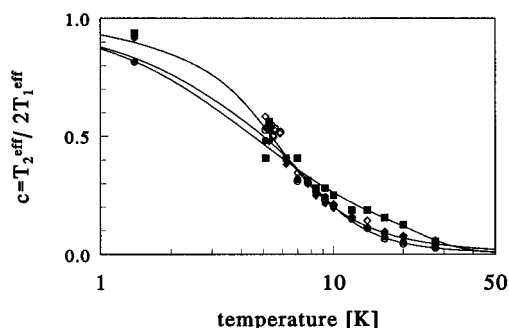


Figure 5. Plot of the coherence parameter c as defined in eq 2 for the lowest excited states, determined from Figure 3a. Markers correspond to those of Figure 3a.

would be substantially higher this crossing over into incoherent energy transfer would still take place at 5 K. Assuming that proteins of other photosynthetic antenna systems will display similar dynamics represented by transitions within the TLS as those in FMO, it seems that this dephasing mechanism is important as a limiting factor for the coherence of energy transfer in these systems.

Conclusions

Using an accumulated photon echo technique we determined the dephasing rates of the lowest transitions in the Q_Y region of FMO at temperatures below 30 K. The wavelength dependence of the observed dephasing time constants can be qualitatively understood in terms of downward energy transfer within the Q_Y manifold. A temperature study showed that at the lowest temperatures the most important dephasing mechanism is the coupling of the individual pigments to so called two level systems which might reflect different conformational substates in the protein. At higher temperatures activation of transitions to higher electronic levels within the manifold seems to be the main mechanism for additional dephasing of the transitions. Although the longest time constants for dephasing as determined with this technique are affected by spectral diffusion, we have been able to make an estimation of the temperature at which coherent energy transfer crosses over into incoherent energy transfer. In FMO, this limiting temperature is mainly determined by the dephasing due to transitions within TLS. Since the strength of the coupling between the pigments and the TLS will be comparable in various pigment–protein complexes, it might be expected that this limiting temperature for coherent energy transfer will be roughly the same for other pigment–protein complexes with similar physical parameters (dipolar interaction energies between the individual pigments, disorder, etc.).

Acknowledgment. We thank S. C. M. Otte and C. Francke for help in the isolation of the FMO-complex. This work was supported by the Life Science Foundation (SLW), financed by the Netherlands Organization for Scientific Research (NWO).

References and Notes

- (1) Kenkre, V. M.; Reineker, P. *Exciton Dynamics in molecular crystals and Aggregates*; Springer-Verlag: Berlin, 1982.
- (2) Rahman, T. S.; Knox, R. S.; Kenkre, V. M. *Chem. Phys.* **1979** *44*, 197.
- (3) Knox, R. S.; Gülen, D. *Photochem. Photobiol.* **1993** *57*, 40.
- (4) Kenkre, V. M. *Phys. Lett.* **1978** *65A*, 391.
- (5) McDermott, G.; Prince, S. M.; Freer, A. A.; Hawthornthwaite-Lawless, A. M.; Papiz, M. Z.; Cogdell, R. J.; Isaacs, N. W. *Nature* **1995** *374*, 517.
- (6) Kuhlbrandt, W.; Wang, D. N.; Fujiyoshi, Y. *Nature* **1994** *367*, 614.
- (7) Matthews, B. W.; Fenna, R. E. *Acc. Chem. Res.* **1980** *13*, 309.

- (8) Tronrud, D. E.; Schmidt, M. F.; Matthews, B. W. *J. Mol. Biol.* **1986** *188*, 443.
- (9) Gudowska-Nowak, E.; Newton, M. D.; Fajer, J. *J. Phys. Chem.* **1990** *94*, 5795.
- (10) Thorn-Leeson, D.; Berg, O.; Wiersma, D. A. *J. Phys. Chem.* **1994** *98*, 3913.
- (11) Thorn-Leeson, D.; Wiersma, D. A. *Phys. Rev. Lett.* **1995** *74*, 2138.
- (12) Meijers, H. C.; Wiersma, D. A. *Chem. Phys. Lett.* **1991** *181*, 312.
- (13) Meijers, H. C.; Wiersma, D. A. *Phys. Rev. Lett.* **1992** *68*, 381.
- (14) Olson, J. M. In *The photosynthetic bacteria*; Clayton, R. K.; Sistrom, W. F., Eds.; Plenum Press: New York, 1978; p 161.
- (15) Vasmel, H.; Swarthoff, T.; Kramer, H. J. M.; Amesz, J. *Biochim. Biophys. Acta* **1983** *725*, 361.
- (16) Swarthoff, T.; Amesz, J.; Kramer, H. J. M.; Rijgersberg, C. P. *Isr. J. Chem.* **1981** *21*, 332.
- (17) van Mourik, F.; Verwijst, R. R.; Mulder, J. M.; van Grondelle, R. *J. Phys. Chem.* **1994** *98*, 10307.
- (18) Pearlstein, R. M. *Photosynth. Res.* **1992** *31*, 213.
- (19) Lu, X.; Pearlstein, R. M. *Photochem. Photobiol.* **1993** *57*, 86.
- (20) Louwe, R. J. W.; Vrieze, J.; Aartsma, T. J.; Hoff, A. J. Submitted.
- (21) Causgrove, T. P.; Yang, S.; Struve, W. S. *J. Phys. Chem.* **1988** *92*, 6790.
- (22) Lyle, P. A.; Struve, W. S. *J. Phys. Chem.* **1990** *94*, 7338.
- (23) Savikhin, S.; Zhou, W.; Blankenship, R. E.; Struve, W. S. *Biophys. J.* **1994** *66*, 110.
- (24) Gillbro, T. In *Green Photosynthetic Bacteria*; Olson, J. M., Ormerod, J. G., Amesz, J., Stackebrand, E., Truper, H. G., Eds.; Plenum Press: New York, 1988; p 91.
- (25) Zhou, W.; LoBrutto, R.; Lin, S.; Blankenship, R. E. *Photosynth. Res.* **1994** *41*, 89.
- (26) Savikhin, S.; Struve, W. S. *Photosynth. Res.* **1996** *48*, 271.
- (27) Johnson, S. G.; Small, G. J. *J. Phys. Chem.* **1991** *95*, 471.
- (28) Miller, M.; Cox, R. P.; Olson, J. M. *Photosynth. Res.* **1994** *41*, 97.
- (29) Aartsma, T. J.; Louwe, R. J. W.; Schellenberg, P. In *Advances in photosynthesis*; Amesz, J., Hoff, A. J., Eds.; Kluwer Academic Publishers: Dordrecht, 1995; Vol. 3, p 109.
- (30) Nuijs, A. M.; van Grondelle, R.; Joppe, H. L. P.; van Bochove, A. C.; Duysens, L. N. M. *Biochim. Biophys. Acta* **1985** *810*, 94.
- (31) Beechem, J. M. In *Methods in Enzymology*; Academic Press: New York, 1992; Vol. 210, p 37.
- (32) Saikan, S.; Nakabayashi, T.; Kanematsu, Y.; Tato, N. *Phys. Rev. B* **1988** *38*, 7777.
- (33) Louwe, R. J. W.; Aartsma, T. J. *J. Luminescence* **1994** *58*, 154.
- (34) Louwe, R. J. W.; Aartsma, T. J. In *Photosynthesis: from light to biosphere*; Mathis, P., Ed.; Kluwer Academic Publishers: Dordrecht 1995; Vol. I, p 363.
- (35) Hesselink, W.; Wiersma, D. A. *Chem. Phys. Lett.* **1978** *56*, 227.
- (36) Schellenberg, P.; Louwe, R. J. W.; Shochat, S.; Gast, P.; Hoff, A. J.; Aartsma, T. J. In *Photosynthesis: from light to biosphere*; Mathis, P., Ed.; Kluwer Academic Publishers: Dordrecht, 1995; Vol. I, p 819.
- (37) Jankowiak, R.; Tang, D.; Small, G. J.; Seibert, M. *J. Phys. Chem.* **1989** *93*, 1649.
- (38) Völker, S. In *Relaxation processes in molecular excited states*; Fünfschilling, J., Ed.; Kluwer Academic Publishers: Dordrecht, 1989; p 113.
- (39) Jackson, B.; Silbey, R. *Chem. Phys. Lett.* **1983** *99*, 331.
- (40) Boxer, S. G.; Gottfried, D. S.; Lockhart, D. J.; Middendorf, T. R. *J. Chem. Phys.* **1987** *86*, 2439.
- (41) Hoff, A. J.; Vasmel, H.; Lous, E. J.; Amesz, J. In *Green Photosynthetic Bacteria*; Olson, J. M., Ormerod, J. G., Amesz, J., Stackebrand, E., Truper, H. G., Eds.; Plenum Press: New York, 1988; p 119.
- (42) Louwe, R. J. W.; Aartsma, T. J. In preparation.
- (43) Bai, Y. S.; Fayer, M. D. *Chem. Phys.* **1988** *128*, 135.
- (44) Bai, Y. S.; Fayer, M. D. *Phys. Rev. B* **1989** *39*, 11066.
- (45) Jankowiak, R.; Small, G. J. In *The Photosynthetic reaction center*; Deisenhofer, J., Norris, J. R., Eds.; Academic Press: San Diego, 1993; Vol. II, p 133.
- (46) Neerken, S.; Franken, E. M.; Aartsma, T. J. In preparation.
- (47) Vulto, S. I. E.; Streltsov, A.; Aartsma, T. J. *J. Phys. Chem.* **1997** *101*, 4845.
- (48) Lee, H. W. H.; Patterson, F. G.; Olson, R. W.; Wiersma, D. A.; Fayer, M. D. *Chem. Phys. Lett.* **1982** *90*, 172.
- (49) van der Laan, H.; Smorenburg, H. E.; Schmidt, Th.; Völker, S. J. *Opt. Soc. Am. B* **1991** *9*, 931.
- (50) Littau, K. A.; Elschner, A.; Fayer, M. D. *Chem. Phys. Lett.* **1990** *175*, 149.
- (51) Lee, H. W. H.; Fayer, M. D. *J. Chem. Phys.* **1986** *84*, 5463.
- (52) Morsink, J. B. W.; Wiersma, D. A. *Chem. Phys. Lett.* **1982** *89*, 291.
- (53) Wannemacher, R.; Koedijk, J. M. A.; Völker, S. *Chem. Phys. Lett.* **1993** *206*, 1.
- (54) Meijers, H. C. Ph.D. Thesis, University of Groningen, The Netherlands, 1994.